Nuclear Instruments and Methods in Physics Research A 669 (2012) 79–84

Contents lists available at SciVerse ScienceDirect

Nuclear Instruments and Methods in Physics Research A

journal homepage: www.elsevier.com/locate/nima

Investigation of a lithium foil multi-wire proportional counter for potential ^{3}He replacement

Kyle A. Nelson*, Steven L. Bellinger, Benjamin W. Montag, James L. Neihart, Todd A. Riedel, Aaron J. Schmidt, Douglas S. McGregor

S.M.A.R.T. Laboratory, Mechanical and Nuclear Engineering, Kansas State University, Manhattan, KS 66506, USA

ARTICLE INFO

Article history:
Received 5 October 2011
Received in revised form
16 November 2011
Accepted 2 December 2011
Available online 9 December 2011

Keywords:
^{3}He replacement
Neutron detection
Lithium foil

ABSTRACT

The recent shortage in the supply of ^{3}He for neutron detection has caused a large surge in research for a viable replacement. ^{6}Li has a large cross section for the absorption of thermal neutrons and emits two relatively short-ranged interaction products. Li foil can now be manufactured thin enough to allow both reaction products to escape the foil. Ten layers of natural Li foil were placed in a multi-wire continuous flow gas chamber with a single anode wire between each foil. Four different thicknesses, 30, 50, 75 and 120 μm, were tested in a thermalized neutron beam. The intrinsic thermal neutron detection efficiencies of 10 layers of 30, 50, and 75 μm thick Li foil were measured to be 8.1, 11.1, and 15.7 percent. The n/γ ratio was found to be 1.25×10^7 using a ^{137}Cs gamma-ray source. Additionally, neutron response pulse-height spectra of the four foil thicknesses are presented and compare well to simulated response spectra. Theoretical calculations show that thermal neutron detection efficiencies above 70 percent are achievable using enriched ^{6}Li foils for the same detector geometries.

1. Introduction

^{3}He proportional counters are commonly used for neutron detection and are critical to nuclear safeguards, homeland security, and oil well exploration and logging. In recent years, ^{3}He has reached a supply crisis and a significant amount of research has been initiated to find and/or develop a realistic alternative. The requirements for the replacement of ^{3}He neutron detectors are high thermal neutron detection efficiency, large area, and high gamma-ray discrimination. Current commercially available alternatives, such as boron-lined counters and BF_3 proportional counters, have limitations and fail many of the requirements to replace established ^{3}He proportional counting systems. These limitations include poor efficiency, low gamma-ray discrimination, and some of the newer designs would require a complete replacement of the electronics and structure already in place at certain facilities and locations. Several neutron reactive materials, such as ^{6}Li, ^{10}B, ^{113}Cd, and ^{157}Gd, and have been used as neutron detectors [1–13]. However, the focus can be narrowed to ^{6}Li and ^{10}B materials due to the large reaction *Q*-value and short ranges of their reaction products. In the present work, natural Li foils are being investigated, which only contain 7.5 percent ^{6}Li, due to its commercial availability. The thermal neutron (0.0259 eV) microscopic cross section for ^{6}Li is 940 b and the ^{6}Li(n,t)^{4}He reaction leads to the following products, with a reaction *Q*-value of 4.78 MeV,

$$^6\mathrm{Li}+{}^1_0n\rightarrow{}^3\mathrm{H}(2.73\,\mathrm{MeV})+\alpha(2.05\,\mathrm{MeV}).$$

For slow neutron absorptions, the reaction products are emitted in opposite directions (180°).

Thin-film coated devices, such as boron-coated semiconductor diodes and boron-lined proportional counters, are limited to low efficiency due to reaction product self-absorption [14]. Further, because the reaction products are emitted in opposite directions, one may enter the detecting medium, be it gas, scintillator or semiconductor, but the other reaction product will not. For a gas-filled detector, the other reaction product will enter the wall onto which the coating was applied. This "wall effect" causes the loss of substantial energy, and therefore, a reduced signal-to-noise ratio and reduced gamma-ray discrimination.

Therefore, using a device where both reaction products can be measured simultaneously becomes critical. One adaptation to the coated diode devices is to add microstructures to the surface, which has been researched extensively [15,16]. The microstructures allow both reaction products to be measured simultanesouly, thereby, increasing the detection efficiency by an order of magnitude as compared to common thin-film coated planar diodes.

New ultra-thin Li foil fabrication technology has matured in the Li battery industry. The Li foils ranging in thickness from 30–120 μm are routinely manufactured. Note that the range

* Corresponding author.
E-mail address: knelson1@ksu.edu (K.A. Nelson).

0168-9002/$ - see front matter © 2011 Elsevier B.V. All rights reserved.
doi:10.1016/j.nima.2011.12.003

of 2.73 MeV ^{6}Li(n,t)^{4}He reaction tritons is 134 μm in pure Li metal, and the range of 2.05 MeV alpha particle reaction products is 23.3 μm [14]. Hence, Li foils can be acquired with thickness of the order or less than the ^{6}Li(n,t)^{4}He reaction product ranges. Suspending ultra thin Li foil in a gas-filled chamber and positioning an anode wire on either side of the foil will allow the device to measure both reaction products simultaneously. By stacking several ultra-thin foils with alternating anode wires positioned between the foils, a large area high-efficiency neutron detector can be realized, without the use of ^{3}He gas. Additionally, if the foils were produced from enriched ^{6}Li metal, the intrinsic thermal neutron detection efficiency could match or exceed that of ^{3}He proportional counters, depending on the number of foils used and the thickness of the foils. Furthermore, Li is a low-*Z* material and a relatively low density solid, which reduces the probability of absorbing gamma-rays.

In the present work, theoretical calculations are compared to experimental results. Measured intrinsic thermal neutron detection efficiency results of 30, 50, and 75 μm thick foils corroborate the theoretical efficiency plots. The Li foil multi-wire proportional counter also has high gamma-ray discrimination with insignificant loss of thermal neutron detection efficiency. Experimentally obtained ^{6}Li(n,t)^{4}He reaction pulse-height spectra of 30, 50, 75, and 120 μm thick Li foil samples are compared to simulated results of the same thicknesses.

2. Theoretical considerations

The calculated efficiencies expected from a multi-wire Li foil detector design are discussed in the following section. Also included is a short discussion on thermal neutron detection efficiency calibration and pulse height spectra modeling.

2.1. Operation and efficiency calculations

Shown in Fig. 1 is a conceptual arrangement for a multi-foil multi-wire proportional counter with an inset of a single foil [17]. Because the range of the triton reaction product is longer than the thicknesses of the Li foil, the triton has a high probability of escaping the foil. There is a minute chance that neither reaction product will escape the foil, and that probability will increase with foil thickness. Because the summed range of the interaction products is much longer than the thickness of the Li foil, there is a chance that the reaction products will escape both sides of the Li foil, thereby, leaving more energy in the chamber than a conventional coated proportional counter. As the interaction products travel through the gas medium, they deposit their energy and generate free electron-ion pairs. The electrons travel to the central anode wire where the device operates as a conventional proportional counter by creating a Townsend avalanche [3,4]. The ions travel to the cathode of the chamber, which can be either the metal casing or the grounded Li foil, because both are conductive metals.

The theoretical calculations performed to obtain the intrinsic thermal neutron detection efficiency of the natural Li foils have been developed elsewhere and are well understood [14]. The analytical approach, using a system of equations, allows for calculations of neutron detection efficiencies for thin-film coated diode devices having various neutron absorber layers and layer thicknesses [14]. Although originally developed for coated semiconductor diodes, the same equations can be used for gas-filled detectors.

Using the method in the literature, and allowing for attenuation of neutrons through each foil, efficiency calculations were performed using the density of natural Li, 0.531 g/cm^{3}, and an energy threshold or lower level discriminator (LLD) setting of 300 keV. The macroscopic thermal neutron absorption cross section is 3.25 cm^{-1} for natural Li. Eventually, the detector will be designed with enriched ^{6}Li foils, in which case the density of enriched ^{6}Li metal is 0.460 g/cm^{3}, although and the range of the triton and alpha particles are nearly unchanged at 134 μm and 23.3 μm, respectively. The macroscopic thermal neutron absorption cross section is 43.56 cm^{-1} for pure ^{6}Li. Shown in Figs. 2 and 3 are the results of the theoretical calculations for 1–5, 10, 15, and 20 foils, ranging in thickness from 1–180 μm for natural and enriched Li foils. The plots show that for a particular number foils there is an optimum thickness of the foils that maximizes the intrinsic thermal neutron detection efficiency. Note also that the calculations assume the incident neutrons are perpendicular to the faces of the foils as shown in the conceptual arrangement in Fig. 1.

The experimental neutron detection efficiency of the multi-wire proportional counter was calculated using three measurements. The first measurement, *a*, was obtained using just the multi-wire proportional counter placed in a collimated neutron beam. The second measurement, *b*, was collected from a ^{3}He proportional counter positioned behind the multi-wire detector, but still in the neutron beam. The last measurement, *c*, was again collected from the ^{3}He proportional counter, but the multi-wire

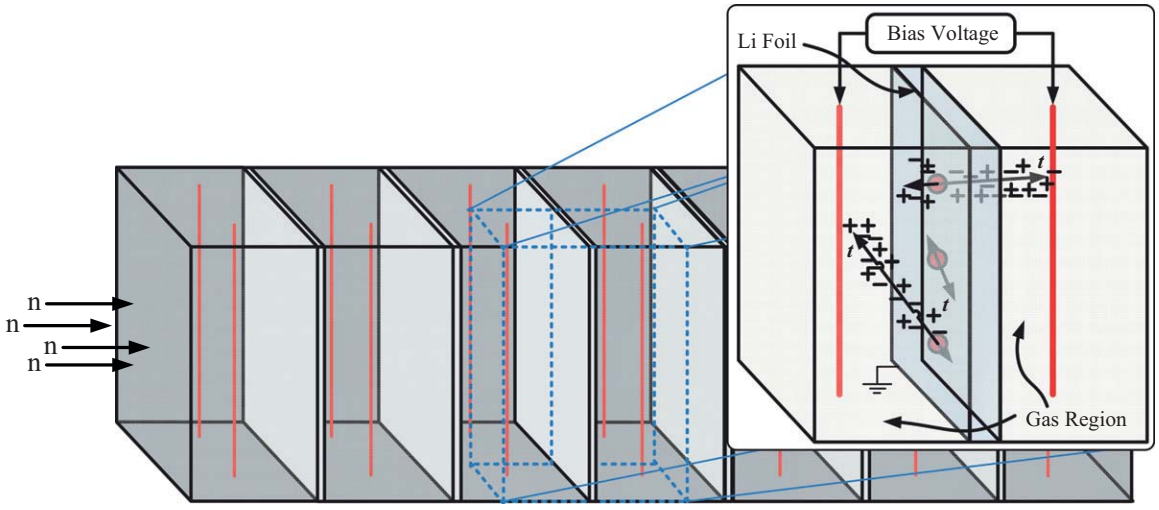

Fig. 1. A cross-sectional illustration of a portion of the conceptual arrangement of the Li foil multi-wire proportional chamber.

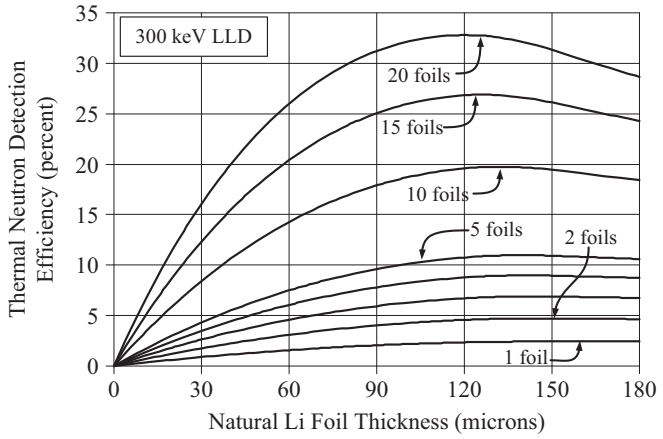

Fig. 2. Thermal neutron detection efficiency as a function of natural Li foil thickness and number of layers. The foil thicknesses are the same for each different layering number.

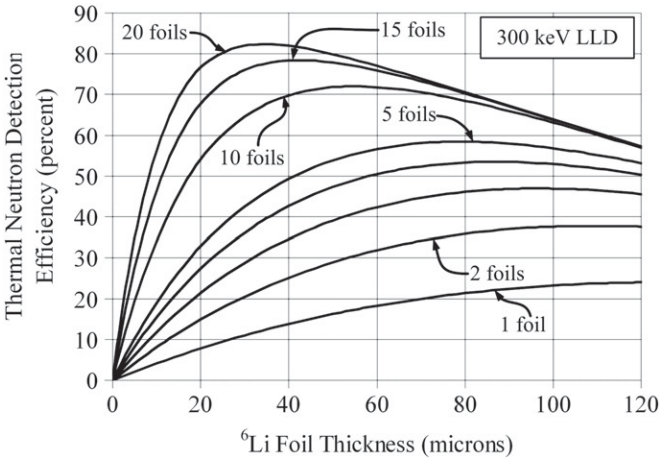

Fig. 3. Thermal neutron detection efficiency as a function of enriched ^{6}Li foil thickness and number of layers.

detector was positioned out of the neutron beam while the ^{3}He detector remained in place. The thermal neutron detection efficiency can be calculated using the following equations.

$$\left(1-\frac{b}{c}\right) = \text{neutron attenuation} \tag{1}$$

$$\left(\frac{a}{c-b}\right) = \text{neutron fraction} \tag{2}$$

Eq. (1) is the fraction of neutrons absorbed by the multi-wire detector. Eq. (2) is the fraction of the neutrons that are absorber and counted by the multi-wire detector. Thus, the intrinsic thermal neutron detection efficiency can be calculated by multiplying (1) and (2) together. If the ^{3}He tube used does not have a 100 percent thermal neutron detection efficiency, $\varepsilon_{^{3}\mathrm{He}}$, the detector efficiency, $\varepsilon_{\mathrm{det}}$, becomes:

$$\left(1-\frac{b}{c}\right)\left(\frac{a}{c-b}\right)\varepsilon_{^{3}\mathrm{He}} = \varepsilon_{\mathrm{det}} \tag{3}$$

The thermal neutron detection efficiency can also be calculated using (4). However, when developing a new detector, it is helpful to know the neutron attenuation of the device, which is given by (1). For example, a detector could absorb 90 percent of the neutrons that transmit through it, but only have an intrinsic neutron detection efficiency of 10 percent. Eq. (1) can be used to examine the detector properties, thereby, adding valuable understanding of the detector and its capabilities.

$$a\left(\frac{c}{\varepsilon_{^{3}\mathrm{He}}}\right)^{-1} = \varepsilon_{\mathrm{det}} \tag{4}$$

2.2. Simulated neutron response pulse-height spectrum

The neutron reaction product energy-deposition spectra were developed using a Monte Carlo simulation implementing the methodology developed elsewhere [18,19]. For the simulation, it was assumed that the gas medium was transparent to neutrons and was therefore ignored. It was also assumed that all the energy deposited in the gas would contribute to the pulse height. A uniformly distributed, 1 cm diameter collimated thermal neutron beam, was centered on a 17 cm by 17 cm ^{6}Li foil sheet. Centering the beam allows the entire energy of the triton to be absorbed in the gas without the interaction product escaping the boundary of the simulation. The range of the triton in P-10 gas (90 percent Ar, 10 percent CH_4) is 7.26 cm. The beam dimensions and energy were chosen to resemble the diffracted thermal neutron beam at the Kansas State University (KSU) TRIGA Mark II nuclear reactor. Hence, a direct comparison can be made between the experimental Li foil pulse-height spectra and the simulated spectra.

All modeled spectra were simulated with a single pure ^{6}Li foil. A ^{6}Li foil macroscopic cross section, Σ, of 43.56 cm^{-1} was calculated using a density of 0.463 g/cm^3 and used to obtain an absorption distribution function through the thickness of the foil. The triton and alpha particles were emitted in opposite directions. Stopping power functions of both the triton and alpha particle in pure ^{6}Li and P-10 gas were obtain using SRIM and were incorporated into the simulation [20]. A random angle of trajectory was selected for the interaction products and any particle reaching the edge of the foil with more than 10 keV of energy was recorded. A histogram plot of the number of interactions versus energy deposited in P-10 gas was developed. The histogram represents the expected pulse-height distribution, which was estimated as a Gaussian distribution and smeared to resemble the expected resolution of a gas-filled proportional detector. The resulting energy spectra for 30, 50, 75, and 120 μm thicknesses of Li foil are shown in Fig. 4. Notable spectral features include the large peak, contributed mostly from the triton energy, and the large dip in the lower energy region. Additionally, for thinner Li foils, there is a small shoulder appearing to the right of the large main peak, occurring when energy from both interaction products contribute

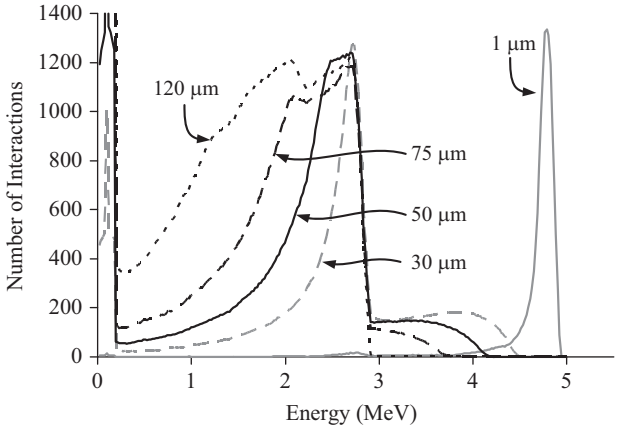

Fig. 4. The neutron response simulation results of 1, 30, 50, 75, and 120 μm thick ^{6}Li foils.

to a single pulse. An additional 1 μm thick ^{6}Li foil is presented in the simulation results in Fig. 4. The 1 μm thick foil is a benchmark to show that the simulation functioned properly. Almost the entire Q-value of 4.78 μMeV can be collected from a 1 μm thick Li foil, well in agreement with the simulation. Note, the simulated pulse-height spectra were adjusted to have relatively similar counts in the most pronounced peak to assist with energy correlations to reaction product energies.

3. Experimental procedure

Three rolls of natural Li foil from Honjo Metals, being 30, 50, and 75 μm thick and 50 mm wide, along with a 120 μm thick by 50 mm wide natural Li foil from American Elements, were opened in an argon glovebox. The foil was laid in the center of a 15 cm by 15 cm Al frame and fastened into position using conductive copper tape. The remaining 5 cm on top and bottom of the foil was covered with aluminum foil to prevent any electronic cross-talk between adjacent anode wires, but did not cover any of the Li foil. Ten frames, with the Li foil, were placed in a continuous flow gas chamber 16 cm by 16 cm by 45 cm spaced 4.5 cm apart with a 25 μm thick tungsten anode wire positioned down the center of the spacing between each foil, with the walls of the chamber at each end. A small plastic chassis lining the side of the chamber was used to fix the frames upright. The chassis did not interfere with any of the neutron or gamma-ray measurements.

Because the distance between foils in the larger box is shorter than the range of the triton in P-10 gas, an additional smaller chamber was used to obtain a more accurate neutron response spectrum. The dimensions of the smaller chamber allow the entire triton energy to be absorbed in the gas without colliding into any structures in the chamber. Although a spectrum was obtained with the larger box, its main use was to obtain an intrinsic efficiency of a Li foil multi-wire proportional counter. After the chambers were loaded and sealed, the valves were closed and the door to the glovebox was opened. P-10 gas was connected to the chambers and set to a high flow rate to prevent any oxygen from entering the chambers. The boxes were placed in the collimated thermalized neutron beam at the KSU TRIGA Mark II nuclear reactor where pulse-height spectra were collected in 600 s intervals. Note that prior to loading the Li foil, pulse-height counting curves were obtained in order to find the ideal operating voltage bias, which was 300 V for the larger chamber and 350 V for the smaller chamber.

To obtain the neutron detection efficiency of the larger chamber, a 600 s pulse-height spectrum was collected at a reactor power of 1 kW. Channel number 45 was used as the LLD for calculating the thermal neutron detection efficiency. The ^{3}He tube was placed behind the box and another 600 s long measurement was collected from the ^{3}He tube to measure the thermal neutron attenuation of the multi-wire foil detector. An additional 600 s measurement was collected using the ^{3}He tube, with the larger chamber removed from the neutron beam. The three measurements above were applied to Eq. (3) to find the intrinsic thermal neutron detection efficiency, and subsequently compared to the theoretical calculations. Additionally, the neutron response spectra of the 30, 50, 75 and 120 μm thick Li foil samples from the smaller chamber are presented and compared to the simulated spectra.

An additional experiment was performed investigating the gamma-ray sensitivity using the larger chamber with 10 layers of 75 μm thick Li foils. A 71.8 mCi ^{137}Cs gamma-ray source was placed directly in front of the 15 cm by 15 cm face so that gamma-rays were emitted parallel to the length of the chamber. Another thermal neutron detection efficiency calculation was performed to eliminate all gamma-ray interactions in the lower channel numbers by setting the LLD to channel number 80. In addition, an n/γ ratio was calculated at both LLD settings.

4. Experimental results

The spectra obtained from the 30, 50, 75, and 120 μm thick Li foil in the smaller chamber are shown in Figs. 5–8. For thicker foils, more reaction product self absorption occurs and smaller energy pulses begin to build up in the lower channel numbers. However, there is a significant valley between the main energy peak (near channel number 400) and the electronic noise. The

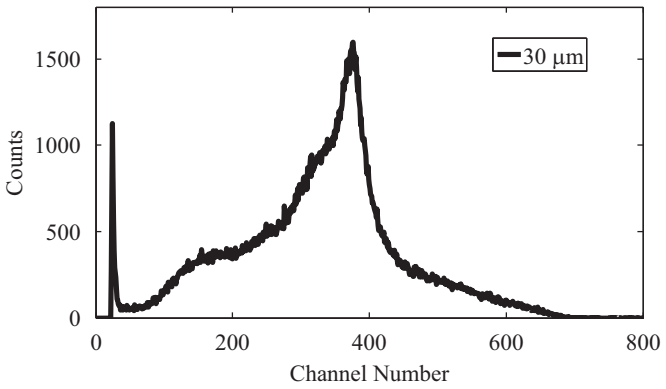

Fig. 5. The neutron response spectrum of a single Li foil 30 μm thick.

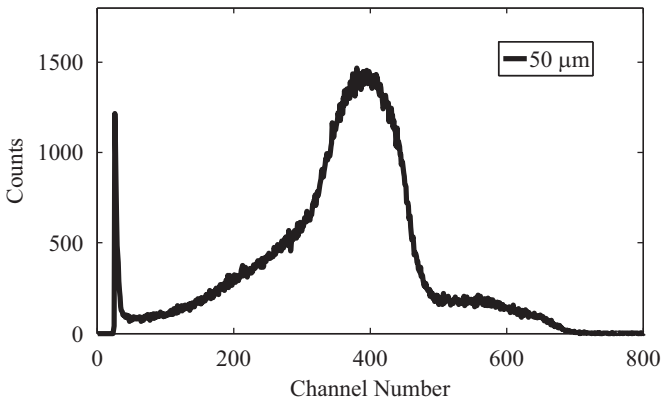

Fig. 6. The neutron response spectrum of a single Li foil 50 μm thick.

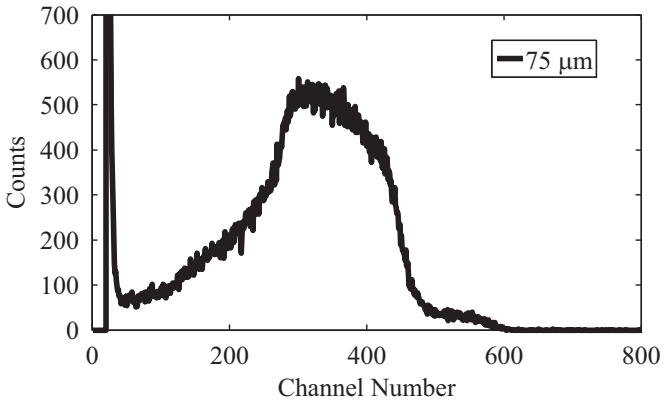

Fig. 7. The neutron response spectrum of a single Li foil 75 μm thick.

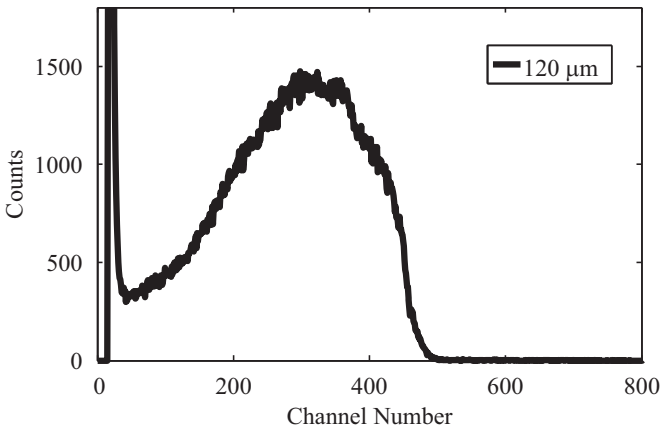

Fig. 8. The neutron response spectrum of a single Li foil 120 μm thick.

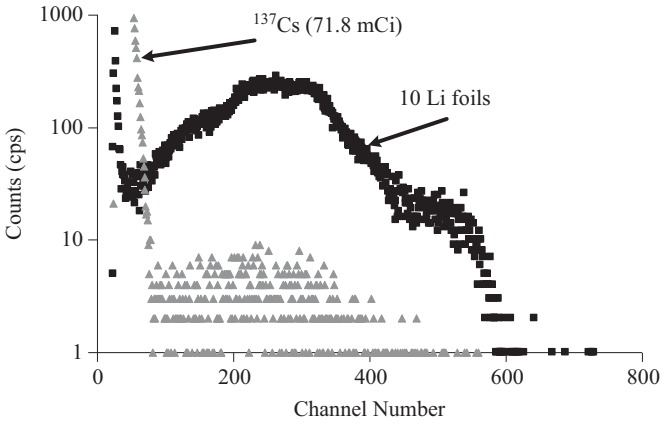

Fig. 9. The gamma ray response of the large chamber with 10 layers of 75 μm thick Li foil compared to the neutron response of the same foils and chamber.

intrinsic thermal neutron detection efficiencies of the 10 layers of 30, 50, and 75 μm thick Li foil were calculated to be 8.1, 11.1, and 15.7 percent, respectively.

The gamma-ray detection efficiency was calculated and used to find the n/γ ratio. The gamma-ray pulse-height spectrum collected from the large chamber is shown in Fig. 9 with the neutron response spectrum of the 10 layers of 75 μm thick foil. The LLD used in the gamma ray experiment was channel number 45, which resulted in an n/γ ratio of 5.96×10^6. The large drop in counts near channel number 450 appears similar to the simulated spectra. The edge at channel number 450 correlates to the triton energy at 2.73 MeV. Using this correlation, channel number 45 is equivalent to 273 keV. With the LLD was set to channel 80, approximately 485 keV, thereby, eliminating all the gamma-ray interactions in the lower channel numbers, the n/γ ratio was 1.25×10^7. The interactions in the channel numbers higher than channel 80 during the gamma ray experiment are from albedo neutrons scattering in the reactor bay as the reactor was still at 300 kW of power during the experiment.

5. Discussion

The pulse-height spectra of the 30, 50, 75, and 120 μm thick Li foil all have large valleys between the main peak and the electronic noise, which is excellent for gamma-ray discrimination as shown by the n/γ ratio. The LLD can be adjusted to a high energy setting with negligible loss in neutron detection efficiency. The intrinsic thermal neutron detection efficiency decreased from 15.7 to 15.3 percent, when the LLD was raised from approximately 273 keV to 485 keV equivalent. The measured n/γ ratio is higher than that of ^{3}He proportional counters at 1×10^5 [21]. The 75 μm thick foil has the highest gamma-ray interaction probability of the three 10 layer foil experiments performed, mainly because there is more absorber material. Thus, it is valid to assume the n/γ ratio will increase for thinner foils. This speculation is supported by both the experimental and simulation results, in which both show a decrease in the number of counts in the lower channel numbers as the foil thickness decreases.

The spectra acquired using the small chamber resembles the expected result from a prototype pressurized chamber with ^{6}Li foils. The spectra from the large chamber appeared similar, but there was an extra feature appearing near channel number 300. The extra feature was a result of triton collisions with adjacent foils, thereby depositing less energy in the gas. Increasing the pressure of the chamber would decrease the range of the triton to allow all the energy to be entirely absorbed in the gas.

The calculated intrinsic thermal neutron detection efficiency of the 10 layers of natural Li foil compared well to the values of the theoretical calculations plotted in Fig. 2. Thus, assuming the ^{6}Li thermal neutron detection efficiency theoretical calculations to be correct, fabricating a detector with 70 percent thermal neutron detection efficiency would require 10 layers of foil approximately 55 μm thick. Additionally, using 20 layers of 30 μm thick ^{6}Li foil would maximize the neutron detection efficiency at 82 percent.

6. Conclusions

The shortage of ^{3}He for large-area neutron detection has caused a substantial drive in research for a viable replacement. Here is shown the potential for ^{6}Li foils to replace ^{3}He detectors. The results of natural Li foils have been compared to theoretical calculations, allowing for predicted performance with the use of ^{6}Li enriched foils. Additionally, making these detectors is uncomplicated, and Li foils can be acquired in rolls that can stretch over several meters. Future work consists of making large area (1×1 m) chambers using ^{6}Li foils in a planar pattern. Alternate patterns to prevent neutron streaming will also be investigated. Finally, the results show that the gamma-ray discrimination ability of the Li foil detector exceeds that of present day ^{3}He detectors.

Acknowledgments

This work was supported in part by DTRA. The authors express their gratitude to the KSU TRIGA Mark II nuclear reactor staff for their helpful assistance.

References

[1] W. Price, Nuclear Radiation Detection, 2nd Edition, McGraw-Hill, New York, 1964.
[2] P. Convert, J.B. Forsyth, Position-Sensitive Detection of Thermal Neutrons, Academic Press, New York, 1983.
[3] N. Tsoulfanidis, Measurement and Detection of Radiation, 2nd Edition, Taylor and Francis, New York, 1995.
[4] G.F. Knoll, Radiation Detection and Measurement, 3rd Edition, Wiley, New York, 2000.
[5] B. Feigl, H. Rauch, Nuclear Instruments and Methods 61 (1968) 349.
[6] T. Aoyama, Y. Oka, K. Honda, C. Mori, Nuclear Instruments and Methods A 314 (1992) 590.
[7] A. Mireshghi, G. Cho, J. Drewery, T. Jing, S.N. Kaplan, V. Perez-Mendez, D. Wildermuth, IEEE Transactions on Nuclear Science NS-39 (1992) 635.
[8] A. Mireshghi, G. Cho, J.S. Drewery, W.S. Hong, T. Jing, H. Lee, S.N. Kaplan, V. Perez-Mendez, IEEE Transactions on Nuclear Science NS-41 (1994) 915.

[9] F. Foulon, P. Bergonzo, A. Brambilla, C. Jany, B. Guizard, R.D. Marshall, Proceedings of MRS 487 (1998) 591.
[10] A.G. Vradii, M.I. Krapivin, L.V. Maslova, O.A. Matveev, A.Kh. Khusainov, V.K. Shashurin, Soviet Atomic Energy 42 (1977) 633.
[11] D.S. McGregor, J.T. Lindsay, R.W. Olsen, Nuclear Instruments and Methods A 381 (1996) 498.
[12] M.A. Lone, R.A. Levitt, D.A. Harrison, Atomic Data and Nuclear Data Tables 26 (1981) 511.
[13] J.K. Tuli, Thermal-neutron-capture gamma rays, BNLNCS-51647 Report, UC-34-C, Brookhaven National Laboratory, Upton, 1983.
[14] D.S. McGregor, M.D. Hammig, Y.-H. Yang, H.K. Gersch, R.T. Klann, Nuclear Instruments and Methods A 500 (2003) 272.
[15] D.S. McGregor, W.J. McNeil, S.L. Bellinger, T.C. Unruh, J.K. Shultis, Nuclear Instruments and Methods, A 608 (2009) 125.
[16] J.K. Shultis, D.S. McGregor, Nuclear Instruments and Methods, A 606 (2009) 608.
[17] S.L. Bellinger, W.J. McNeil, K.A. Nelson, M.F. Ohmes, D.S. McGregor, Gas-filled neutron detector having improved detection efficiency, PCT/US2010/046736, 2010.
[18] J.K. Shultis, D.S. McGregor, Proceedings of SPIE 7079 (2008) 06:1.
[19] S.L. Bellinger, W.J. McNeil, T.C. Unruh, D.S. McGregor, IEEE Transactions on Nuclear Science **NS-56 56** (2009) 742.
[20] J. Ziegler, J. Biersack, Stopping Ranges of Ions in Matter (SRIM), Version 2008.
[21] PANDA:, D. Reilly, N. Ensslin, H. Smith Jr., S. Kreiner, Passive Nondestructive Assay of Nuclear Materials, U.S. Government Printing Office, Washington, D.C, 1991 380.